

Evaluation of Cutting Temperature and Optimization in Milling of GGG60 Cast Iron

Rasit Duzce¹ , Gurcan Samtas^{2*} 

¹ Düzce University, Department of Manufacturing Engineering, Graduate School of Education, 81620, Düzce, Türkiye

² Düzce University, Department of Mechatronics Engineering, Faculty of Engineering, 81620, Düzce, Türkiye

Abstract

Spheroidal graphite cast irons have increased ductility, tensile strength, and toughness compared to other cast irons. Additionally, it can be mentioned that choosing spheroidal graphite cast iron over steel material has a better machining feature. In this study, face milling operations were carried out using GGG60 material and different inserts, feed, and depth of cut. The Taguchi method was used for the experimental design, and 27 experiments were performed. During the experiments, a thermal camera measured the temperature from the cutting zone. Experimental results were evaluated with analysis of variance and graphics, and cutting parameters were optimized. As a result of the optimization, optimum parameters for minimum temperature, TiAlN coated insert, 300 m/min cutting speed, 0.30 mm/tooth feed rate, and 0.5 mm depth of cut were found. According to the results obtained from the study, the most influential parameter affecting the temperature was the cutting speed. In addition, the TiAlN-coated insert has been observed as the most suitable coating type for minimum temperature.

Keywords: GGG60, Face milling, Taguchi, Optimization, Cutting temperature.

Cite this paper as:

Duzce, R. and Samtas, G. (2024).
Evaluation of Cutting Temperature and Optimization in Milling of GGG60 Cast Iron. Journal of Innovative Science and Engineering, 8(1): 63-77

*Corresponding author: Gurcan Samtas
E-mail: gurcansamtas@duzce.edu.tr

Received Date: 27/10/2022

Accepted Date: 18/04/2024

© Copyright 2024 by
Bursa Technical University. Available
online at <http://jise.btu.edu.tr/>



The works published in Journal of Innovative Science and Engineering (JISE) are licensed under a Creative Commons Attribution-NonCommercial 4.0 International License.

1. Introduction

Cast irons can be produced more efficiently in addition to their mechanical properties such as hardness, wear resistance, machinability, corrosion resistance, and strength. They have widely used engineering materials because they are economical [1]. Cast irons' machining depends on the casting's type and microstructure. While machining white cast iron is difficult, ferritic casting is more accessible than other cast irons. The machinability of spheroidal graphite cast iron, vermicular graphite cast iron, and alloyed and tempered cast irons are between white and ferritic castings [2]. Nodular graphite cast irons are used in many sectors, such as mining, machinery manufacturing, agricultural products, transportation, and construction. The mechanical properties of these materials are pretty good, and their corrosion resistance is high. Generally, cast irons are brittle. Spheroidal graphite cast irons, on the other hand, have an extremely tensile structure [3].

The surface quality of the material under processing is adversely affected by deformations in the cutting tools used in machining. The loss of tool life is the most significant of these drawbacks. One of the most important elements determining the cost of the cutting tools, or the production expenses, is the shortening of their lifespan. Therefore, it is important to know the parameters affecting tool life and to develop measures to control them [4]. Good mechanical properties are one of the most critical factors distinguishing it from other materials. In addition, the machining of the material is as necessary as the mechanical properties. Improving the machining of engineering materials is an industrially important parameter as it will reduce manufacturing costs.

As a result, several studies on machining can be found in the literature. When the literature is analyzed, certain studies claim that the alloying elements added to the material significantly impact the microstructure, mechanical characteristics, cutting force, and surface roughness of ductile cast iron and austempered ductile cast iron [5, 6]. Again, in some studies, it is stated that low austempering temperature decreases the surface roughness values while increasing the cutting forces in the machining of spheroidal graphite cast iron and austempered spheroidal graphite cast iron. It has also been stated that increasing the cutting speed reduces the vibration during the cutting process [7, 8]. In addition, various studies investigate the abrasive wear behaviour of austempered spheroidal graphite cast irons, the effect of cooling in the austempering process, and the effect of austempering temperature and time on machining [9-11]. Moncada et al. investigated the parameters affecting the machinability in turning austempered cast irons [12]. The wear types that occur in cutting tools in cast iron machining are abrasive, adhesive, and diffusion wear. The cutting tool properties sought in cast iron machining are high hardness and chemical stability. Besides sintered carbides, ceramic cutting tools are also used in cast iron machining [13]. Marwanga et al., in the turning process, investigated the changes in the microstructure of cast irons during machining [14]. Ahmet et al. Their study investigated the effect of machining conditions and material structure on the stress between the pencil and the part in the turning of four different lamellar graphite cast irons. Their study determined that the most significant factor in the stress difference increase was the amount of graphite in the total cross-section [15]. Kaçal et al. investigated the cutting tool wear and surface roughness during GGG70 ductile cast iron milling. According to the test results, it was observed that the surface roughness increased with the increase of the feed rate [16]. Kahraman et al., In their study, investigated the effect of austempering temperature and time on the surface roughness in the milling of vermicular graphite cast irons. In their research, they observed that the austempering heat treatment improved the surface quality of the materials [17]. Çakıroğlu and Uzun, in their study, performed the modeling

of the cutting force and workpiece surface roughness in the milling of vermicular graphite cast irons with artificial neural networks. As a result of the obtained mathematical model, it was seen that there was a harmony between the predicted values and the experimental results [18]. Askun et al., In their study, evaluated the machinability of spheroidal graphite cast irons alloyed with Ni and Cu in terms of cutting forces and surface qualities [19]. Avishan et al. investigated the effect of depth of cut on the machinability of alloyed austempered cast iron. As a result of their studies, they stated that reducing the depth of cut would not improve machinability [20]. Saraswati et al. investigated the mechanical properties and drillability behaviour of glass-sisal-epoxy hybrid composite material containing fillers such as fly ash and graphene. In addition, the mechanical and physical properties of the composite material used in their studies, such as tensile, bending, impact resistance, hardness, density and water absorption percentage, were also examined [21]. Pradhan et al. machined complex-shaped tapered holes using hot, abrasive jet machining. In their work, they conducted experimental studies to evaluate the abrasive footprint effect for hot, abrasive jet machining on surface roughness. They also modelled experimental studies using computational fluid dynamics [22]. Mahapatra et al. applied a hard turning process to AISI H13 steel using nanofluid with a minimum quantity of lubrication. The experiments measured tool vibration and surface roughness and analyzed chip morphology. In the experiments, AlTiNSiN nanocomposite-coated cutting tools were used [23]. Pradhan et al. performed the turning process on Functionally Graded material using nano-fluid-assisted minimum amount lubrication, and the machined surface and chip morphology were examined. In their study, they used three different spindle speeds, three different feeds and three different cutting depths. They chose the Taguchi L27 orthogonal array for the experimental design. Microstructure images of the machined surfaces were also examined with a scanning electron microscope [24]. Jena et al. applied hard turning to high-strength, low-alloy AISI 4340 steel. Their study modelled the surface roughness and optimized the cutting parameters. For the experimental design, the Taguchi L16 orthogonal array was selected. According to the ANOVA analysis performed in the study, it was stated that feed rate and cutting speed were effective parameters on surface roughness [25]. HAJM (Hot Abrasive Jet Machining) is a non-traditional process in which heated abrasive particles are sprayed at high speed and pressure. Pradhan et al. Their study applied the HAJM machining process, which uses SiC abrasive parts, to S_3N_4 material. In the study, regression models were created for all experimental results. The microstructures of the part surfaces after processing were analyzed using a scanning electron microscope. Additionally, CFD simulation was used, and RSM and genetic algorithms were also used [26].

When the literature was examined, no study was found to examine the cutting temperatures and evaluate the effects of cutting parameters in the face milling process of GGG60 material. In addition, the article has a unique value in using the Taguchi methodology in this study. In the study, L27 (3^4) Taguchi orthogonal array was chosen. Instead of 81 full factorial designs, 27 experiments were performed [27]. Experimental results were evaluated with Analysis of Variance (ANOVA) and 3D graphics. In addition, Taguchi's predictive values and experimental outcomes were compared.

2. Material and Methods

This article investigated the effects of cutting parameters on the cutting temperature in the face milling process of GGG60 cast iron, and the cutting parameters were optimized using the Taguchi method. The recommended dimensions for the test sample to be milled according to the ISO 8688-1 standard are at least three times the length and 0.6 times the cutting width of the tool holder diameter used [28]. Considering this situation, specially cast GGG60 spheroidal graphite cast iron was used in the milling experiments. The technical specifications of GGG60 cast iron are shown in Tables 1 and 2.

Table 1. GGG60 cast iron components (Matweb)

C	Fe	Mn	P	S	S
%3.2	%92.83	%0.1	%.0.15-	%	%0.005

Table 2. Mechanical and physical properties of GGG60 cast iron (Matweb)

Intensity	Hardness Brinell	Tensile Strength
7.30 g/cm ³	200-270	550 Mpa

In the experiments, TN6525 coded TiAlN coated, TN7535 coded TiN-TiCN-Al₂O₃ coated, and WS30PM coded AlTiN (multilayer) coated four cutting edge cutting edges belonging to WIDIA (Germany) cutting tool company were used. In addition, the three-edged tool holder suitable for the tips used is specially produced and supplied as an equivalent. (Figure 1).

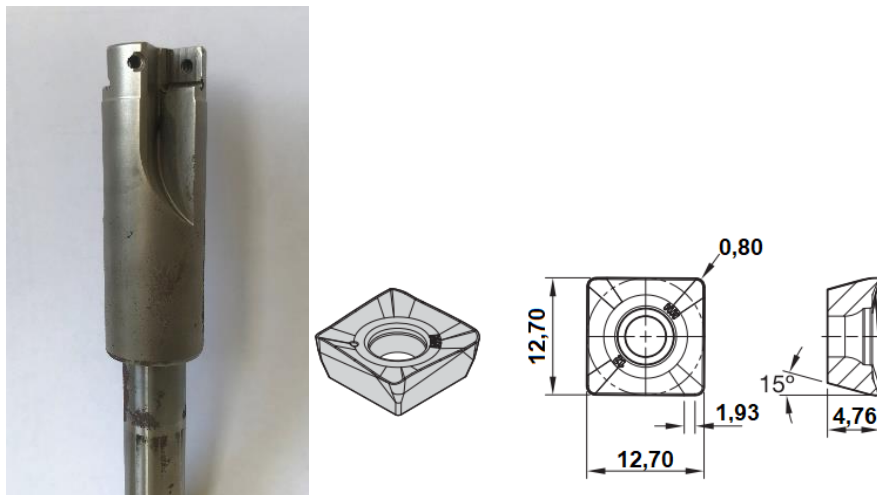


Figure 1. Tool holder and insert used

DELTA SEIKI 1050A triaxial vertical milling machine was used in milling operations. Experiments were performed in a dry environment without using a cooling liquid. Temperature measurements were made with a Fluke TiS20 thermal imager when the cutting tool reached the midpoint of the material. This takes about 3 seconds. The thermal camera used can measure between -20 °C and 350 °C, has a detector resolution of 120x90, a field of view of 35.7° x 26.8°, and a frame rate of 9 Hz.

3. Taguchi Method

3.1. Design and Conduct of Experiments

The Taguchi L27 orthogonal array was used for the experimental design. Only 27 experiments were performed instead of the full factorial design of 81 experiments. The number of experiments can be drastically reduced when using the Taguchi technique for analysis and assessment. To identify quality features, the Taguchi approach makes use of several functions. The Taguchi “smaller the better” function was used in this study because the smallest value was desired for the cutting zone temperature measurements. The selected cutting parameters and their levels are given in Table 3. The cutting tool catalogue was considered in determining the cutting parameters [29, 30]. The experimental design was created by considering the L27 orthogonal array. The experimental results and the S/N (signal-to-noise) ratios calculated according to the experimental results are given in Table 4.

Table 3. Parameters and levels

Parameters	Level 1	Level 2	Level 3
Cutting inserts (Kt)	TiAlN	TiN-TiCN-Al ₂ O ₃	AlTiN
Cutting speed (V, m/dak)	175	225	300
Feed rate (f, mm/tooth)	0.10	0.20	0.30
Cutting depth (a, mm)	0.5	1	1.5

Table 4. Experimental design and measured temperature values

Exp. no	Cutting parameters				Experimental results and S/N ratios	
	A	B	C	D	Temperature (T, °C)	S/N _T (dB)
	Cutting inserts (Kt)	Cutting speed (V)	Feed rate (f)	Cutting depth (a)		
1	TiAlN	175	0.1	0.5	47.7	-33.570
2	TiAlN	175	0.1	0.5	55.9	-34.948
3	TiAlN	175	0.1	0.5	54.9	-34.791
4	TiAlN	225	0.2	1	57.8	-35.239
5	TiAlN	225	0.2	1	54.3	-34.696
6	TiAlN	225	0.2	1	61.8	-35.820
7	TiAlN	300	0.3	1.5	52.7	-34.436
8	TiAlN	300	0.3	1.5	55.3	-34.855
9	TiAlN	300	0.3	1.5	48.4	-33.697
10	TiN-TiCN-Al ₂ O ₃	175	0.1	1.5	49.9	-33.962
11	TiN-TiCN-Al ₂ O ₃	175	0.1	1.5	57.6	-35.208
12	TiN-TiCN-Al ₂ O ₃	175	0.1	1.5	55.7	-34.917
13	TiN-TiCN-Al ₂ O ₃	225	0.2	0.5	58	-35.269
14	TiN-TiCN-Al ₂ O ₃	225	0.2	0.5	55	-34.807
15	TiN-TiCN-Al ₂ O ₃	225	0.2	0.5	57.1	-35.133
16	TiN-TiCN-Al ₂ O ₃	300	0.3	1	58.2	-35.298
17	TiN-TiCN-Al ₂ O ₃	300	0.3	1	58.8	-35.388
18	TiN-TiCN-Al ₂ O ₃	300	0.3	1	60.4	-35.621
19	AlTiN	175	0.1	1	53.4	-34.551
20	AlTiN	175	0.1	1	67.4	-36.573
21	AlTiN	175	0.1	1	66.8	-36.496

22	AlTiN	225	0.2	1.5	57.7	-35.224
23	AlTiN	225	0.2	1.5	52.7	-34.436
24	AlTiN	225	0.2	1.5	50.2	-34.014
25	AlTiN	300	0.3	0.5	47.7	-33.570
26	AlTiN	300	0.3	0.5	45.6	-33.179
27	AlTiN	300	0.3	0.5	51	-34.151

According to the test results, the average value of the temperature results was calculated as 55.259 °C, and the average S/N ratio for the temperature was -34.809 dB. The graph of the temperature values obtained from the experiments is given in Figure 2.

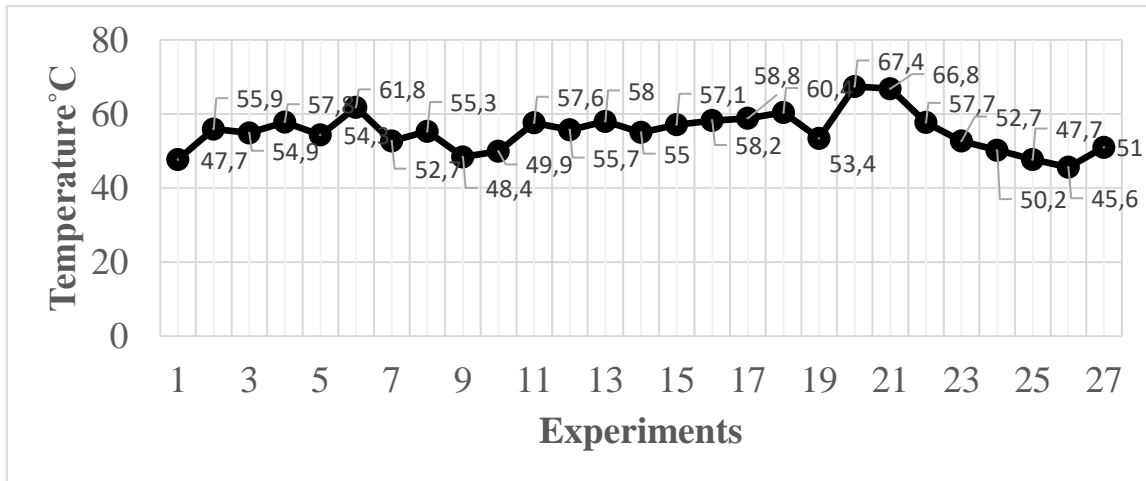


Figure 2. Temperature values obtained from experiments

The temperature images taken with the thermal camera are shown in Figure 3. The highest value in the cutting zone was considered in temperature measurements. In the study, it is seen that the highest temperature was in the 20th experiment. Here, the low feed rate also increases the machining time of the cutting tool on the material. Therefore, long friction is thought to cause an increase in temperature. On the other hand, AlTiN coatings have a higher coefficient of friction than different coating types. Therefore, the temperature increase in the 20th experiment can also be attributed to the coating type.

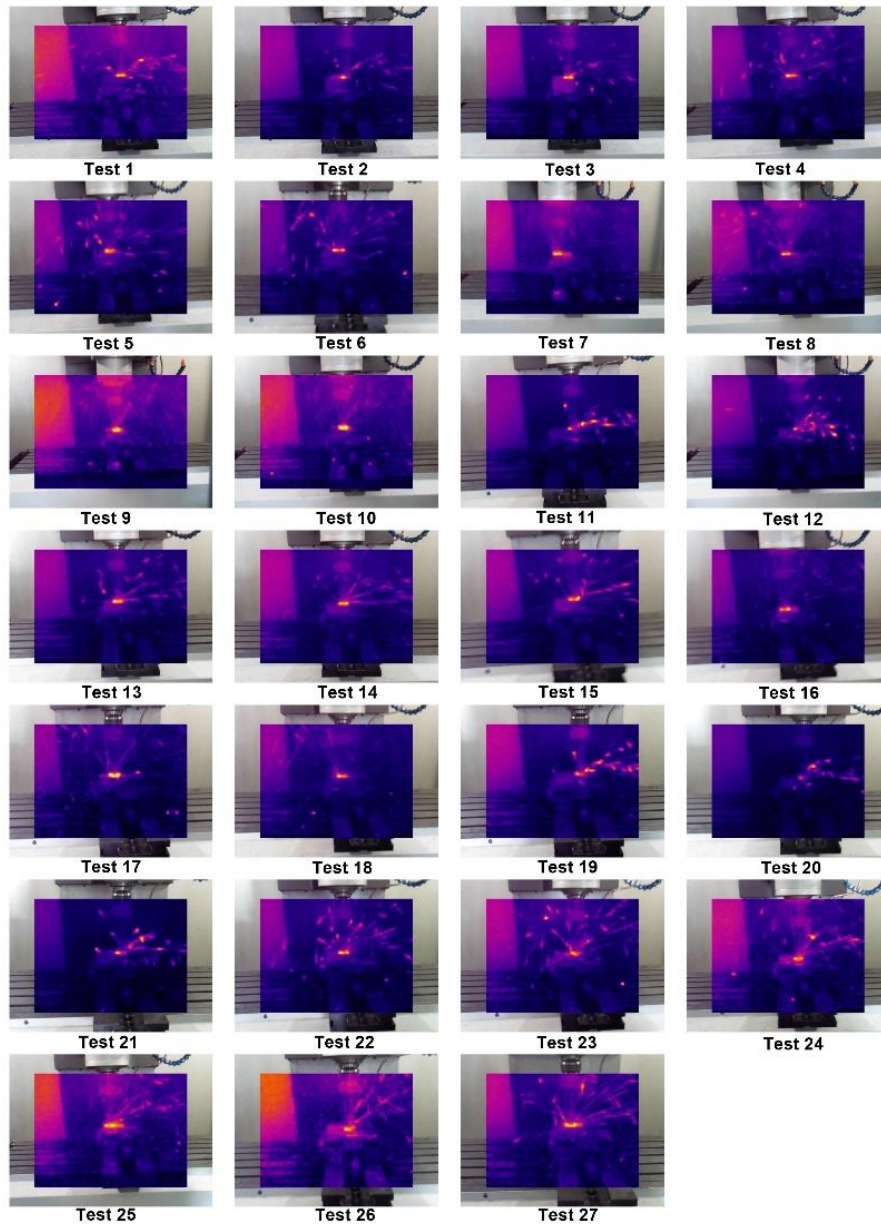


Figure 3. Thermal images obtained with a thermal camera

3.2. Determining Optimum Levels

Table 5 shows the averages of the S/N ratios for each level. These levels show the average values of the S/N ratios calculated for the analysis of temperature values in the experimental research. Predictive values for the ideal parameters are computed using these values.

Table 5. Means of S/N ratios for each level

Parameters	Levels			Delta
	Level 1	Level 2	Level 3	
A (Cutting insert, Kt)	-34.70	-35.08	-34.74	0.38
B (Cutting speed, V)	-35.06	-34.98	-34.48	0.58
C (Feed rate, f)	-35.06	-34.98	-34.48	0.58
D (Cutting depth, a)	-34.40	-35.56	-34.56	1.16

One of the critical steps in the Taguchi method is specifying the optimum levels. Optimum levels are determined by evaluating different levels of cutting parameters and combinations created by the chosen orthogonal array. These levels are used to draw the effect graph (Figure 4). At the same time, they were evaluating the main effect graph. The lowest level for the temperature values and the highest levels for the S/N ratios are considered since the desired minimum temperature.

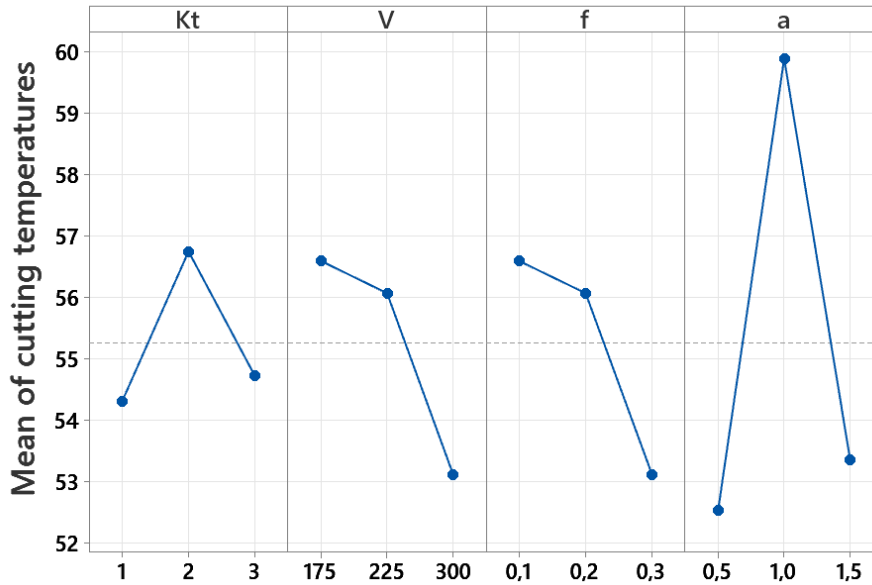


Figure 4. Main effect graph for temperature values

The optimum combination of test parameters for minimum temperature values according to Figure 2 is $A_1B_3C_3D_1$ (A_1 = TiAlN coated insert, B_3 = 300 m/min cutting speed, C_3 = 0.30 mm/tooth feed rate and D_1 = 0.5 mm cutting depth) determined.

3.3. Evaluation by ANOVA

The Taguchi confidence interval is calculated using an ANOVA (Analysis of Variance) to examine the interactions between all the parameters employed in the experimental design, how they affect the quality characteristics, how these changes in quality characteristics occur at various cutting parameter levels [31, 32]. The effects of the cutting insert, cutting speed, feed rate, and depth of cut on temperature were evaluated by ANOVA, and the results of the ANOVA are shown in Table 6.

Table 6. ANOVA results

Factors	Degrees of freedom (DF)	Sum of squares (SS)	Mean squares (MS)	F	T-Value	P-Value	Factor effect (%)
Kt	1	0.761	0.7606	0.02	0,16	0.877	0.10
V	1	58.456	8.8007	0.29	-0,53	0.599	7.84
f	1	4.425	4.4246	0.14	0,38	0.708	0.59
a	1	2.961	2.9606	0.10	0,31	0.760	0.40
Error(e)	22	678.543	30.8429				91.06
Total	26	745.145					100

According to the ANOVA result, the R^2 value was 8.94%. When the variance analysis results were evaluated, the most influential parameter affecting the temperature was the cutting speed, with 7.84%. This parameter is followed by the

rate of progression of 0.59%. The error rate in the table is 91.06%. The amount of an observed variable differs from the model's predicted value in ANOVA. So, the error is the portions of the scores not accounted for by the analysis. In ANOVA, the errors are assumed to be independent and generally distributed around the sample means [33]. In the Taguchi method, analysis of variance is used to calculate the confidence interval and determine the most influential parameter. Therefore, it is sufficient to state that cutting speed is the most significant factor here. It is also possible to see similar results in the literature [34].

3.4. Confirmation Tests and Taguchi Predicted Values

The validation experiments and the quality characteristics are examined in the final stage of the Taguchi method. To put it another way, validation experiments are run to verify the chosen ideal set of cutting parameters and levels. A₁B₃C₃D₁ (A₁= TiAlN coated insert, B₃ = 300 m/min cutting speed, C₃ = 0.30 mm/tooth feed rate, and D₁ = 0.5 mm depth of cut) estimation based on the optimum combination obtained for the temperature, taking into account the individual effects of the cutting parameters temperature value (T_p) is calculated with the following equations [35, 36].

$$\eta_{gT} = A_1 + B_3 + C_3 + D_1 - 3\eta_{\frac{S}{N}-T} \quad (1)$$

$$T_p = 10^{-\eta_{gT}/20} \quad (2)$$

They are the signal-to-noise ratios of the optimum levels of the A₁B₃C₃D₁ parameters (Table 5). $\eta_{\frac{S}{N}-T}$ is the average of the S/N ratios of the temperature values. S/N ratio calculated for η_{gT} temperature optimum levels and T_p are Taguchi prediction values calculated for temperature. The temperature estimate value calculated using Equation 1 and Equation 2 was 48.05 °C. A confidence interval (CI) is used to compare the result of validation experiments with the predicted value and confirm the “smaller the better” characteristic. The CI (Eq. 3) is the maximum and minimum value, and the accuracy of the validation experiments is tested by comparing the calculated value with the predicted values [35, 36].

$$CI = \sqrt{F_{\alpha:1, V_e} \times V_{ep} \times \left(\frac{1}{n_{eff}} + \frac{1}{r} \right)} \quad (3)$$

In equation 3, F_{α:1}, and the significance level is the F ratio of α, α significance level, 1- α confidence interval, V_e is the degree of freedom of the temperature error according to the variance analysis results. When Table 6 is examined, the degree of freedom of the error is 22. In this case, the 1-22 value from the 95% confidence level F table was 4.30. V_{ep} is again the variance of error according to the ANOVA, r is the number of validation experiments, and n_{eff} is the number of effective measured results [37, 38].

$$n_{eff} = \frac{N}{1 + V_t} \quad (4)$$

In Equation 4, N denotes the total number of experiments (27), and V_t represents the total degrees of freedom (4) of the shearing parameters for which the mean is calculated using Table 6. In this case, the n_{eff} was calculated as 5.4. In this study, considering the optimum combination determined for the temperature, three confirmation experiments were

performed for each. They are considering Eq. 3 and Eq. 4; the CI is 8.29. In using the confidence interval, the Taguchi estimation value calculated for each parameter is added and subtracted with the confidence interval. The mean of the validation experiments should be between these two values. The average of three verification tests conducted for the cutting temperature is 49.17 °C. In this case, for temperature, $(48.05-8.29) < 49.17 < (48.05+8.29) = 39.76 < 49.17 < 56.34$ range was obtained, and confirmation experiments for temperature were performed within the confidence interval. In this case, it can be said that the optimization is successful. Table 7 compares the experimental results with the Taguchi predicted values. Eq.1 and Eq.2 were used to calculate the estimation values. The approximative values and experimental values were close to each other. For confidential statistical analysis, error values should be less than 20% [31].

Table 7. Comparison of optimized and random conditions with predicted values

Levels	Taguchi method		
	Experiment	Prediction	Error (%)
A ₁ B ₃ C ₃ D ₁ (Optimum)	49.17	48.05	2.28
A ₂ B ₁ C ₂ D ₃ (Random)	55.70	57.89	3.78
A ₂ B ₂ C ₃ D ₁ (Random)	57.10	53.16	6.90

In Table 7, the experimental values are compared with the predicted values. It is seen that the error values between the results of the confirmation test and the results obtained by the Taguchi method are less than 20%. In this case, the results obtained from the validation experiments show that the optimization has been carried out successfully.

4. Results and Discussion

The cutting parameters affecting the experimental results and the effects of these parameters on the temperature were evaluated with three-dimensional graphics (Figure 5). Figure 5a shows the impact of cutting speed and inserts on the temperature in the graph. Here, the temperature drop is seen in the TiAlN-coated insert. This situation is similar to Taguchi-optimized values. When evaluated together with the cutting speed, it is seen that the temperature decreases with the cutting speed of 175 m/min, the TiAlN coated insert, the 300 m/min cutting speed, and the AlTiN coated insert. Considering all parameter effects in Taguchi optimization, these drop conditions are expected. Figure 5a shows that the highest cutting temperature is at 175 m/min cutting speed and AlTiN coated insert. In addition, in this graph, it is seen that the temperature increases as the cutting speed increases, but the temperature decreases at 300 m/min cutting speed and AlTiN coated insert. Figure 5b shows the effects of insert and feed rate on temperature. Here again, it is seen that the lowest temperature is in the TiAlN-coated insert. In addition, when evaluated with the feed rate, it can be said that these situations are similar to Taguchi optimized values, where the lowest temperature is 0.10 mm/tooth and 0.30 mm/tooth in the TiAlN coated insert. Figure 5b shows a 0.20 mm/tooth feed rate and a sudden temperature rise in the TiAlN-coated insert. This is attributed to the cutter coating type. Figure 5b shows the highest temperature at the AlTiN-coated insert and 0.10 mm/tooth feed. In addition, 0.30 mm/tooth feed and a sudden temperature drop are observed in the AlTiN-coated insert. If low-temperature values are desired, combinations of 0.30 mm/tooth or 0.10 mm/tooth feed and TiAlN coated insert, 0.30 mm/tooth feed, and AlTiN coated insert can be used.

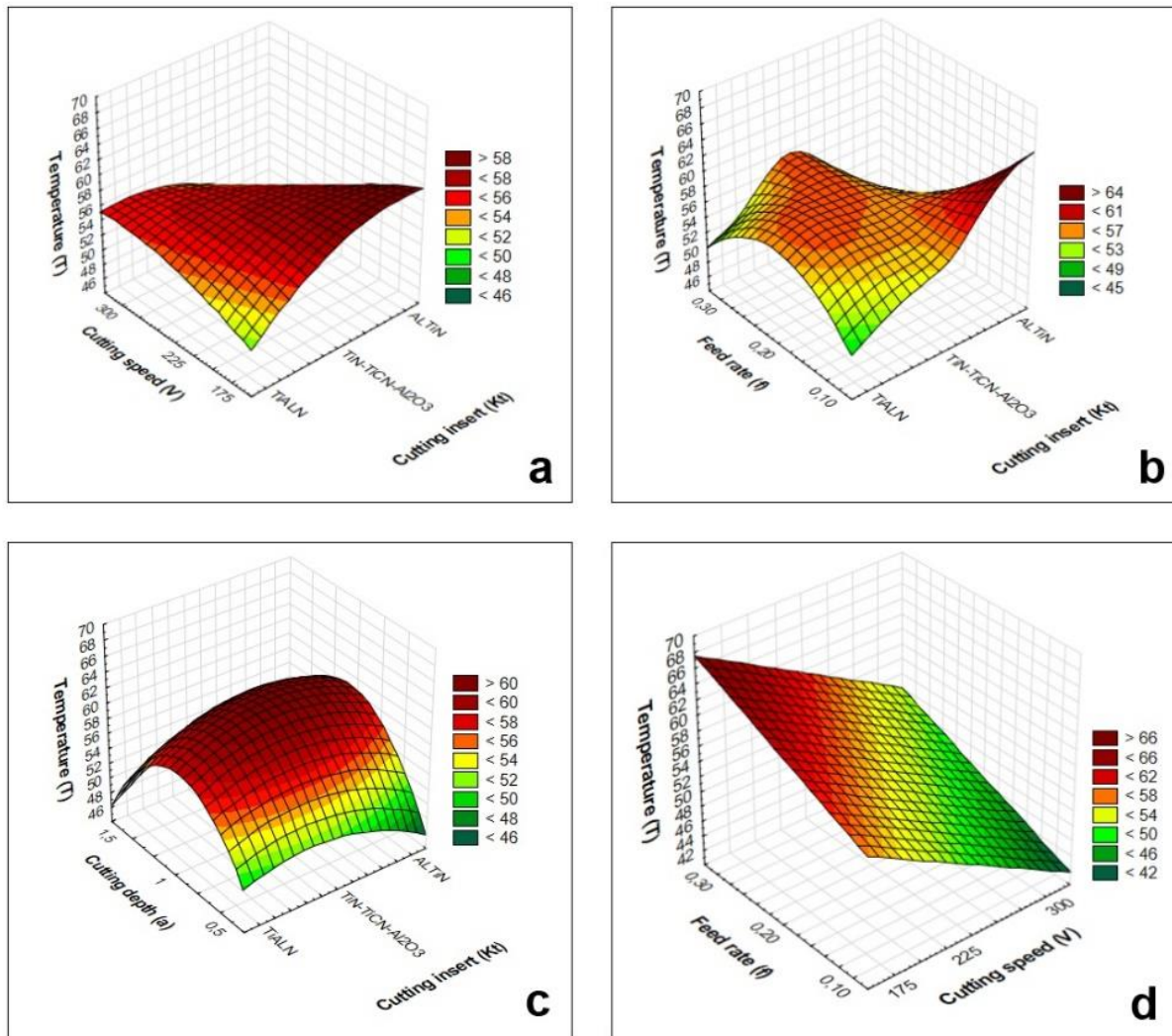


Figure 5. Effects of cutting parameters on temperature

Figure 5c shows the cut depth and the inserts' effects on temperature. Here again, the TiAlN-coated insert showed the best performance. It is seen that the lowest temperature is at 0.5 mm depth of cut and TiAlN insert. This situation is similar to Taguchi's optimized values. In addition, it is seen that the temperature increases as the depth of cut increases but decreases in the combination of 1.5 mm depth of cut and TiAlN insert. It also showed the best performance for all inserts with a depth of cut of 0.5 mm. The effects of cutting speed and feed rate on temperature are shown in Figure 5d. Here, it is seen that the temperature increases as the feed rate increases but decreases as the cutting speed increases. When the cutting speed and feed rate are evaluated together, it can be said that the best performance is 0.30 mm/tooth feed rate and 300 m/min cutting speed, similar to Taguchi's optimized values.

When the graphs were evaluated, it was seen that the TiAlN coating would exhibit ideal performance in terms of temperature in surface milling of GGG60 material. Increasing cutting temperatures during machining may cause chip adhesion to the cutting edge. This will increase the surface roughness. Therefore, low temperature is desired. According to these results, the article has a unique degree in the literature.

5. Conclusions

This study investigated the effects of cutting parameters on the cutting zone temperature in face milling processes applied to GGG60 cast iron. The Taguchi method was used for the experimental design, and 27 experiments were carried out. The cutting parameters were optimized in the study, and three validation experiments were carried out with the optimized parameters after the optimization. Taguchi prediction values and experimental results were compared. In addition, the effects of cutting parameters on temperature were evaluated with three-dimensional graphics. It is possible to list the results obtained from this study as follows;

- As a consequence of the optimization, the optimum combination of the test parameters for the minimum temperature values is $A_1B_3C_3D_1$ (A_1 = TiAlN coated insert, B_3 = 300 m/min cutting speed, C_3 = 0.30 mm/tooth feed rate, and D_1 = 0.5 mm cutting depth).
- The average of the three validation experiments conducted with optimized parameters (49.17 °C) was below the average of the test results (55.259 °C).
- When the variance analysis results were evaluated, the cutting speed was the most influential parameter affecting the temperature, with 7.84%. Since the cutting speed is, the distance travelled in meters per minute, increasing and decreasing the cutting speed directly affects the cutting speed as it will change the friction per unit time. Therefore, the ANOVA result confirms this explanation.
- The estimated value (48.05°C) calculated using the Taguchi method was below the average of the test results. This shows that the Taguchi method can be used successfully in similar studies.
- When the results obtained from the experiments with the optimum and randomly selected parameters were compared with the Taguchi estimation values, the error values were below 7%. For reliable statistics, the error value should be below 20%.
- When the three-dimensional graphics are evaluated, the optimal incision tip coating for the minimum temperature is the TiAlN-coated insert, similar to the Taguchi optimized parameters.
- TiAlN coating is recommended for the inserts used in this study if the low temperature is desired in face milling operations to be applied to GGG60 cast iron.
- Titanium Aluminum Nitride coating is suitable for machining very hard steels, aluminium-silicon and Titanium alloys. This coating thickness is generally 3-5 μm thick. Since it has a very hard structure, it allows work at high speeds. The study results show that this coating is the most ideal for performance.

This study used the Taguchi method to reduce the number of experiments and experimental design, thus saving time and processing costs. As a complete design, instead of 81 experiments, 27 experiments were carried out. When the experimental and Taguchi results are evaluated, the results obtained are applicable and satisfactory. In subsequent studies, tool wear and surface roughness values can be measured in face milling of GGG60 cast iron using the same orthogonal array, and experimental results can be optimized.

References

- [1] Çelik, Ö. (2001). Küresel Grafitli dökme demirlerin aşınma davranışları, Yüksek Lisans Tezi, İstanbul Üniversitesi, Fen Bilimleri Enstitüsü, İstanbul, Türkiye.
- [2] Murthy, V.S.R. and Kishore, Seshan, S., (1984). Characteristics of compacted Graphite Cast Iron, Transactions of the American Foundrymen's Society, 92: 373-380.
- [3] Makine Eğitimi, Küresel grafitli dökme demirler, Erişim Tarihi: Mart 17, 2022 [Online]. Erişim: <https://www.makinaegitimi.com/kuresel-grafitli-dokme-demirler/>.
- [4] Coelho, R.T., Souza, A.F., Roger, A.R., Rigatti A.M.Y. and Riberio, A.A (2010). Mechanistic approach to predict real machining time for milling free-form geometries applying high feed rate, International Journal of Advanced Manufacturing Technology, 46: 1103–1111.
- [5] Hsu, C.H., Chen, M.L. and Hu, C.J. (2007) Microstructure and mechanical properties of 4% cobalt and nickel alloyed ductile irons, Materials Science and Engineering A, 444: 339–346.
- [6] Şeker, U., Çiftçi İ. and Hasirci, H. (2003) The effect of alloying elements on surface roughness and cutting forces during machining of ductile iron, Materials and Design, 24: 47–51.
- [7] Uçun, I. and Aslantas, K. (2009). The performance of ceramic and cermet cutting tools for the machining of austempered ductile iron, International Journal of Advanced Manufacturing Technology, 41: 642–650.
- [8] Ghani, A.K. and Choudhury, Husni I.A. (2002). Study of tool life, surface roughness and vibration in machining nodular cast iron with seramic tool, Journal of Materials Processing Technology, 127: 17–22.
- [9] Klocke, F. Klöpper, C. Lung, D. and Essig, C. (2007). Fundamental wear mechanisms when machining austempered ductile iron (ADI), Annals of the CIRP., 56(1): 73-76.
- [10] Cakir, M.C., Bayram A., Isik, Y. and Salar, B. (2005). The effects of austempering temperature and time onto the machinability of austempered ductile iron, Materials Science and Engineering A, 407: 147–153.
- [11] Çetin, M. ve Gül, F. (2006). Östemperlenmiş küresel grafitli dökme demirin abrasiv aşınma davranışına östemperleme işleminde soğutmanın etkisi, Gazi Üniv. Müh. Mim. Fak. Der., 21(2): 359-366.
- [12] Moncada, O.J., Spicacci, R.H. and Sikora, J.A. (1998). Machinability of austempered ductile iron, AFS Trans, 106: 39–45.
- [13] Çakır, M.C. (2018). Modern Talaşlı İmalatın Esasları, Dora yayınları, 155-239. ISBN: 978-6052470053.
- [14] Marwanga, R.O., Voigt, R.C. and Cohen, P.H. (2000). Influence of graphite morphology and matrix structure on chip formation during machining of continuously cast ductile irons, AFS Transactions, 108: 651, 2000.
- [15] Yardımeden, A., Aksoy, M. ve İnan, A. (2004). Lamel grafitli dökme demirlerin işlenmesinde kale mile parça arasında meydana gelen gerilime, işleme şartları ve malzeme yapısının etkisi, 11. Uluslararası Makina Tasarım ve İmalat Kongresi, Antalya, Türkiye.
- [16] Kaçal, A. Çelik, B. ve Sertsöz, Ş. (2019). GGG70 sfero dökme demirin frezelenmesinde yüzey pürüzlülüğü ve takım aşınmasının incelenmesi, IMCOFE 2019, Antalya, Türkiye, 308-315.
- [17] Kahraman, Y., Uzun, G. ve Korkut, İ. (2015). Vermiküler grafitli dökme demirlerin frezelenmesinde östemperleme sıcaklığı ve süresinin yüzey pürüzlülüğüne etkisi, 6. Ulusal Talaşlı İmalat Sempozyumu (UTİS 2015), İstanbul, Türkiye, 178-188.

- [18] Çakıroğlu, R. ve Uzun, G. (2021). Yüksek ilerleme ile frezeleme işlemi esnasında oluşan kesme kuvvetinin ve iş parçası yüzey pürüzlülüğünün Yapay Sinir Ağları ile modellenmesi, Gazi Mühendislik Bilimleri Dergisi, 7(1): 58-66.
- [19] Aşkun, Y., Hasırcı, H. ve Şeker, U. (2003). Ni ve Cu ile alaşımlandırılmış küresel grafitli dökme demirlerin işlenebilirliğinin kesme kuvvetleri ve yüzey kaliteleri açısından değerlendirilmesi, Pamukkale Üniversitesi Mühendislik Fakültesi, Mühendislik Bilimleri Dergisi, 9(2): 191-199.
- [20] Avishan, B., Yazdani, S. and Jalali, Vahid D. (2009). The influence of depth of cut on the machinability of an alloyed austempered ductile iron, Materials Science and Engineering A, 523: 93-98.
- [21] Saraswati, P.K. Sahoo, S. Parida S.P. and Jena P.C. (2019). Fabrication, characterization and drilling operation of natural fiber reinforced hybrid composite with filler (Fly-Ash/Graphene), International Journal of Innovative Technology and Exploring Engineering, 8 (10): 1653-1659.
- [22] Pradhan, S., Das, S.R., Jena, P.C. and Dhupal, D. (2021). Machining performance evaluation under recently developed sustainable HAJM process of zirconia ceramic using hot SiC abrasives: An experimental and simulation approach, Proceedings of Institute Mechanical Engineering Part C: J Mechanical Engineering Science, 1–27.
- [23] Mahapatra, S., Das, A., Jena, P. C. and Das S.R. (2023). Turning of hardened AISI H13 steel with recently developed S3P-AlTiSiN coated carbide tool using MWCNT mixed nanofluid under minimum quantity lubrication, Proceedings of Institute Mechanical Engineering Part C: J Mechanical Engineering Science, 237(4): 843-864.
- [24] Pradhan, S., Das, S.R., Jena P.C. and Dhupal, D. (2021). Investigations on surface integrity in hard turning of functionally graded specimen under nano fluid assisted minimum quantity lubrication, Advances in Materials and Processing Technologies, 8: 1714-1729.
- [25] Jena, J., Panda, A., Behera, A. K., Jena, P. C., Das, S.R. and Dhupal, D. (2019). Modeling and optimization of surface roughness in hard turning of AISI 4340 steel with coated ceramic tool, Innovation in Materials Science and Engineering, 151-160.
- [26] Pradhan, S., Dhupal, D., Das, S.R. and Jena P.C. (2021). Experimental investigation and optimization on machined surface of Si₃N₄ ceramic using hot SiC abrasive in HAJM, Materials Today: Proceedings, 44: 1877-1887.
- [27] Canıyılmaz, E. ve Kutay, F. (2003). Taguchi metodunda varyans analizine alternatif bir yaklaşım, Gazi Üniv. Müh. Mim. Fak. Der., 18(3): 51-63.
- [28] Taylan, F. (2009). Sert malzemelerin frezelenmesinde takım aşınma davranışlarının belirlenmesi, Doktora Tezi, Süleyman Demirel Üniversitesi, Fen Bilimleri Enstitüsü, Isparta, Türkiye.
- [29] WIDIA Cutting tool company (2020). Advances catalog, WIDIA press, Germany.
- [30] WIDIA Cutting tool company (2017). Master Catalog, WIDIA press, Germany.
- [31] Kara F.(2018). Optimization of surface roughness in finish milling of AISI P20+S plastic-mold steel, Materiali in tehnologije/Materials and technology, 52(2): 195–200.
- [32] Samtaş, G. ve Korucu, S. (2019). Kriyojenik işlem görmüş EN AW 5754 (AlMg3) alüminyum alaşımının frezelenmesinde yüzey pürüzlülüğü için kesme parametrelerinin optimizasyonu, Politeknik Dergisi, 22(3): 665-673.
- [33] Doncaster, C. P. (2022). Terminology of analysis of variance, Accessed: March 18, 2022 [Online]. Available: <http://www.southampton.ac.uk/~cpd/term.html>.

- [34] Samtaş, G. and Korucu, S. (2021). Multiple optimization of cutting parameters in milling of cryogenically treated Aluminium 6061-T651 alloy with cryogenic and normal cutting inserts, *Surface Topography: Metrology and Properties*, 9(4): 1-10.
- [35] Kara, F. and Öztürk, B. (2019). Comparison and optimization of PVD and CVD method on surface roughness and flank wear in hard-machining of DIN 1.2738 mold steel, *Sensor Review*, 39(1): 24-33.
- [36] Kıvak T. (2014). Optimization of surface roughness and flank wear using the Taguchi method in milling of Hadfield steel with PVD and CVD coated inserts, *Measurement*, 50: 19-28.
- [37] Samtaş G. (2015). Optimization of cutting parameters during the face milling of AA5083-H111 with coated and uncoated inserts using Taguchi method, *Int. J. Machining and Machinability of Materials*, 17(3/4): 211-232.
- [38] Samtaş, G. ve Korucu, S. (2019). Temperlenmiş alüminyum 5754 alaşımının frezelenmesinde kesme parametrelerinin Taguchi Metodu kullanılarak optimizasyonu, *Düzce Üniversitesi Bilim ve Teknoloji Dergisi*, 7(1): 45-60.